Available online at www.sciencedirect.com
SCIENCE DIRECT®
PERGAMON
Polyhedron 22 (2003) 989–996
POLYHEDRON
www.elsevier.com/locate/poly

Synthesis, characterization and electrochemical studies of unsymmetrical macrocyclic mono and binuclear nickel(II) complexes

J. Manonmani, M. Kandaswamy *

Department of Inorganic Chemistry, School of Chemical Sciences, Guindy Campus, University of Madras, Chennai 25, India

Received 28 August 2002; accepted 13 January 2003

Abstract

A series of nickel(II) complexes of general formula $[Ni_2L](ClO_4)_2$ with unsymmetrical compartmental macrocyclic ligands was synthesized by stepwise method using 6,6′-piperazine-1,4-diyldimethylenebis(4-X-2-formylphenol) (X = CH_3 or Br), nickel(II) ions and diamines. In this macrocyclic system there are two different N_2O_2 compartments, one has two piperazinyl nitrogens and two phenolic oxygens and the other compartment has two azomethine nitrogens and two phenolic oxygens as coordinating sites. The complexes were characterized by elemental and spectral analysis. The electrochemical properties of the complexes indicate that all the complexes undergo two quasi-reversible one electron transfer processes in the cathodic potential region (0 to −1.3 V) and two quasi-reversible one electron transfer processes in the anodic potential region (0 to +1.3 V). In both reduction and oxidation process the first electron transfer process is shifted towards anodic potential region as the macrocyclic ring size increases. The reduction and oxidation process also changes with the substituent at the *para* position of the phenolic oxygen atoms.

Keywords: Binucleating ligand; Nickel(II) complexes; Electrochemistry

1. Introduction

The chemistry of compartmental ligand capable of forming macrocyclic or acyclic complexes with similar or dissimilar metal ions [1] has become rapidly growing area of research. Of special interest among all other ligand systems, the macrocyclic ligands can impose high degree of preorganisation on metal complex formation. The complexes formed from macrocyclic ligands are used as models [2] for protein–metal binding sites in biological systems, as synthetic ionophores, as therapeutic reagents in chelate therapy for treatment of metal toxication, in catalysis and to investigate the mutual influence of two metal centers on their physicochemical properties [3].

Several types of macrocyclic ligands such as polyazamacrocycles, [4] imine Schiff-base macrocycles [5] and cryptands [6] have been synthesized. Binucleating macrocycles containing two phenolic oxygen as endogenous bridges with symmetrical lateral chains were first prepared by Robson [7]. The symmetrical macrocycles have been extensively used for studies on homobinuclear metal complexes. The disadvantage of the symmetrical compartmental ligands is the process of scrambling of metal ions during the preparation of heterobimetallic complexes. So we decided to prepare unsymmetrical compartmental ligands to avoid the scrambling of metal ions. We have already reported the copper(II) and manganese(III) binuclear phenol based macrocyclic complexes having dissimilar coordination environments with first compartment formed by Mannich base condensation and second compartment formed by Schiff-base condensation [8,9]. The macrocyclic binucleating ligands are shown in Fig. 1. In this work we report the synthesis and studies of unsymmetrical binuclear nickel(II) complexes. The influence of macrocyclic ring size and the *para* substituent to phenoxy oxygen on the spectral and electrochemical properties of the complexes have been studied and discussed.

* Corresponding author. Tel.: +91-44-245-4515; fax: +91-44-235-2494.
E-mail address: mkands@yahoo.com (M. Kandaswamy).

0277-5387/03/$ - see front matter
doi:10.1016/S0277-5387(03)00026-3

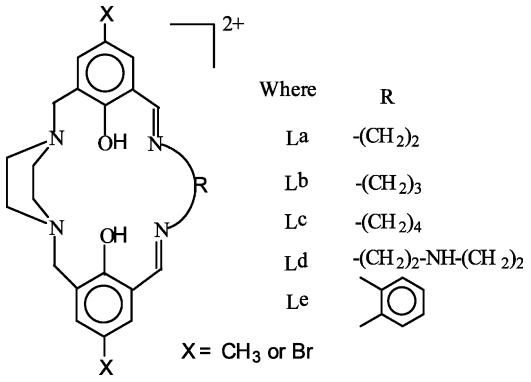

Fig. 1. Macrocyclic binucleating ligand.

2. Experimental

2.1. Physical measurements

C, H, N analysis of the ligands and complexes were carried out using Carlo Erba Model 1106 elemental analyzer. Nickel contents of the complexes were determined by Perkin–Elmer atomic absorption spectrophotometer. ^{1}H NMR spectra (90 MHz) of the ligands were recorded using a FX-80 Q Fourier transform NMR spectrometer. FAB mass spectra of the complexes were recorded on a SX102/DA-6000 mass spectrometer using 3-nitrobenzyl alcohol as the matrix solvent. IR spectra were recorded on a Hitachi-270-50 spectrophotometer in the range 4000–250 cm^{-1}. Electronic spectra were recorded on a Hewlett–Packard 8452A spectrophotometer in the range 250–850 nm. Conductivity measurements were carried out in DMF at 27 °C using CM 82T conductivity bridge (Elcot Pvt. Ltd.). The Cyclic voltammograms were obtained on an apparatus comprising a PAR Model 173 potentiostat/galvanostat, Model 175 universal programmer model 176 current–voltage converter, and model 179 coulometer and a Perkin–Elmer Hitachi 057 $X-Y$ recorder. The electrochemical measurements were carried out in DMF under oxygen free conditions. Platinum foil was used as both working and counter electrodes. Ag/AgCl was used as reference electrodes and tetrabutylammoniumperchlorate (10^{-1} M) was used as supporting electrolyte. The concentrations of complexes are 10^{-3} M. Ferrocenium–Ferrocene(1+) couple was used as an internal standard. All potentials are reported relative to Ag/AgCl reference electrode and the $E_{1/2}$ of the ferrocenium–ferrocene (Fc^+–Fc) couple under the experimental condition is 470 mV in DMF and ΔE_p for Fc^+–Fc is 70 mV at scan rate 50 mV s^{-1}. Controlled potential electrolysis experiments were made on an apparatus comprising a HA-501 potentiostat/galvanostat, a HB-104 function generator and a HF-201 coulomb/amperemeter.

2.2. Materials

5-Methylsalicylaldehyde was prepared by following the literature method [10]. 5-Bromosalicyaldehyde was purchased from Fluka. Tetrabutylammonium perchlorate (TBAP) was obtained from Fluka and recrystallized from methanol. (Caution! All perchlorate salts are explosive and hence care should be taken while handling). DMF (HPLC) was obtained from Qualigens and used as such. All other chemicals and solvents were of reagent grade and used as received.

2.3. Synthesis of precursor compounds

2.3.1. Synthesis of 6,6′-piperazine-1,4-diyldimethylenebis(4-methyl-2-formylphenol) (P.C-I)

The precursor compound (P.C-I) used for the synthesis of macrocyclic complexes was prepared by reported procedure [8].

2.3.2. Synthesis of 6,6′-piperazine-1,4-diyldimethylenebis(4-bromo-2-formylphenol) (P.C-II)

This was prepared by following the above procedure using 5-bromo salicylaldehyde instead of 5-methylsalicylaldehyde.

2.4. Synthesis of complexes

All the homobinuclear complexes were prepared [11] by a stepwise synthesis. Reaction of P.C-I or P.C-II with Ni(II) acetate led to the isolation of mononuclear Ni(II) complex. Further reaction of the complex with 1 equiv. of diamine and 1 equiv. of nickel(II) perchlorate gave the unsymmetrical binuclear complexes Scheme 1.

2.5. Synthesis of mononuclear complexes

2.5.1. [NiL^1] (**1**)

The precursor compound (P.C-I) (3.82 g, 10 mmol) was dissolved in $CHCl_3$–MeOH (45 ml, 1:2) and added to nickel acetate (2.48 g, 10 mmol) dissolved in methanol (30 ml) under boiling condition and refluxed for 1 h. The orange colored precipitate formed was collected by filtration, washed with $CHCl_3$ followed by MeOH and dried. Selected IR data (ν cm^{-1}) (using KBr): 3320, 1670 cm^{-1}.

2.5.2. [NiL^2] (**2**)

This was obtained by following the above procedure using P.C-II with nickel (II) acetate. Selected IR data ν (cm^{-1}) (using KBr): 3330, 1675.

2.5.3. [NiL^{1a}]·H_2O (**3**)

The ethylenediamine (0.064 g, 2 mmol) dissolved in methanol (20 ml) was added to [NiL^1] (0.88 g, 2 mmol) in CH_3CN–MeOH (60 ml, 1:2) under boiling condition.

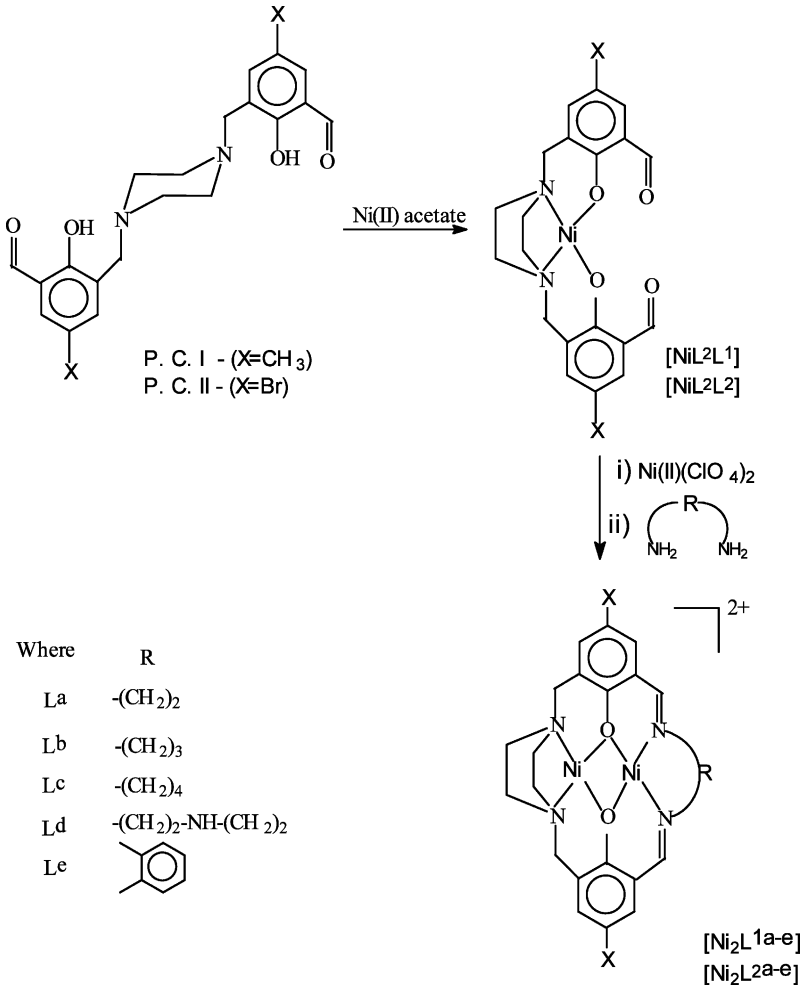

Scheme 1.

A clear solution appeared on addition of ethylenediamine to [NiL[1]] and after sometimes orange colored precipitate appeared. The resulting product was refluxed for 1 h and then the product was collected by filtration, washed with cold MeOH and dried. Selected IR data ν (cm^{-1}) (using KBr): 3340, 1630. *Anal.* Calc. for $C_{24}H_{28}N_4O_2Ni\cdot H_2O$: C, 59.87, H, 6.23; N, 11.64; Ni, 14.13. Found: C, 59.82; H, 6.10; N, 11.58; Ni, 14.09%.

The above procedure was used for the synthesis of the complexes [$NiL^{1b,c}$] and [NiL^{2a-c}].

2.5.4. $[NiL^{1b}]\cdot H_2O$ (4)

Selected IR data ν (cm^{-1}) (using KBr): 3330, 1625. *Anal.* Calc. for $C_{25}H_{30}N_4O_2Ni\cdot H_2O$: C, 60.60, H, 6.46; N, 11.31; Ni, 14.53. Found: C, 60.52; H, 6.42; N, 11.28; Ni, 14.49%.

2.5.5. $[NiL^{1c}]\cdot H_2O$ (5)

Selected IR data ν (cm^{-1}) (using KBr): 3320, 1635. *Anal.* Calc. for $C_{26}H_{32}N_4O_2Ni\cdot H_2O$: C, 61.29, H, 6.68; N, 11.00; Ni, 15.13. Found: C, 61.23; H, 6.52; N, 10.92; Ni, 15.09%.

2.5.6. $[NiL^{2a}]\cdot H_2O$ (6)

Selected IR data ν (cm^{-1}) (using KBr): 3340, 1625. *Anal.* Calc. for $C_{22}H_{22}N_4O_2Br_2Ni\cdot H_2O$: C, 43.28, H, 3.93; N, 9.18; Ni, 9.51. Found: C, 43.22; H, 3.80; N, 9.10; Ni, 9.49%.

2.5.7. $[NiL^{2b}]\cdot H_2O$ (7)

Selected IR data ν (cm^{-1}) (using KBr): 3335, 1625. *Anal.* Calc. for $C_{23}H_{24}N_4O_2Br_2Ni\cdot H_2O$: C, 44.23, H, 4.76; N, 8.97; Ni, 9.29. Found: C, 44.20; H, 4.62; N, 8.88; Ni, 9.22%.

2.5.8. $[NiL^{2c}]\cdot H_2O$ (8)

Selected IR data ν (cm^{-1}) (using KBr): 3320, 1635. *Anal.* Calc. for $C_{24}H_{26}N_4O_2Br_2Ni\cdot H_2O$: C, 45.14, H, 6.38; N, 8.77; Ni, 9.09. Found: C, 45.08; H, 6.22; N, 8.72; Ni, 9.02%.

2.6. Synthesis of binuclear complexes

2.6.1. $[Ni_2L^{1a}](ClO_4)_2\cdot CH_3OH\cdot H_2O$ (L^{1a}–R = –$(CH_2)_2$–) (**9**)

The ethylenediamine (0.15 g, 2 mmol) in methanol (30 ml) was added to [NiL^1] (1.16 g, 2 mmol) in CH_3CN–MeOH (60 ml, 1:2). A clear solution appeared and subsequently nickel perchlorate (0.91 g, 2 mmol) in methanol (30 ml) was added with stirring and refluxed for 2 h. The resulting product was obtained by evaporation of the solvent and collected by filtration, washed with methanol and recrystallized from DMF–MeOH. *Anal.* Calc. for $C_{24}H_{28}N_4O_2Ni_2(ClO_4)_2\cdot CH_3OH\cdot H_2O$: C, 38.95; H, 4.45; N, 7.27; Ni, 15.33. Found: C, 38.98; H, 4.29; N, 7.23; Ni, 15.24%. Selected IR (KBr disc) ν (cm^{-1}): 3350, 1625, 1109. UV–Vis: λ_{max} (nm) ε (M^{-1} cm^{-1}) (DMF): 550 (245), 417 (3603), 335 (4368). Molar conductance [Λ_M, (cm^2 Ω^{-1} mol^{-1})] in DMF: 150.

The procedure adopted for the preparation of [Ni_2L^{1a}] was used for the following binuclear macrocyclic complexes by using the appropriate diamines.

2.6.2. $[Ni_2L^{1b}](ClO_4)_2\cdot H_2O$ (L^{1b}–R = –$(CH_2)_3$–) (**10**)

Anal. Calc. for $C_{25}H_{30}N_4O_2Ni_2(ClO_4)_2\cdot H_2O$: C, 39.33; H, 4.28; N, 7.48; Ni, 15.69. Found: C, 39.96; H, 4.06; N, 7.24; Ni, 15.44%. Selected IR (KBr disc) ν (cm^{-1}): 3483, 1630, 1096. UV–Vis: λ_{max} (nm) ε (M^{-1} cm^{-1}) (DMF): 604 (258), 397 (5135), 350 (6077). Molar conductance [Λ_M, (cm^2 Ω^{-1} mol^{-1})] in DMF: 168. MS (FAB): 534.

2.6.3. $[Ni_2L^{1c}](ClO_4)_2\cdot CH_3OH$ (L^{1c}–R = –$(CH_2)_4$–) (**11**)

Anal. Calc. for $C_{26}H_{34}N_4O_3Ni_2(ClO_4)_2\cdot CH_3OH$: C, 41.53; H, 4.64; N, 7.17; Ni, 15.03. Found: C, 41.25; H, 4.41; N, 7.10; Ni, 15.14%. Selected IR ν (cm^{-1}) (using KBr): 3428, 1630, 1096. UV–Vis: λ_{max} (nm) ε (M^{-1} cm^{-1}) (DMF): 620 (185), 372 (10 480), 285 (sh). Molar conductance [Λ_M, (cm^2 Ω^{-1} mol^{-1})] in DMF: 155.

2.6.4. $[Ni_2L^{1d}](ClO_4)_2\cdot H_2O$ (L^{1d}–R = –$(CH_2)_2$–NH–$(CH_2)_2$–) (**12**)

Anal. Calc. for $C_{26}H_{33}N_5O_2Ni_2(ClO_4)_2\cdot H_2O$: C, 39.94; H, 4.49; N, 8.98; Ni, 15.07. Found: C, 39.88; H, 4.56; N, 8.79; Ni, 14.84%. Selected IR ν (cm^{-1}) (using KBr): 3321, 1625, 1100. UV–Vis: λ_{max} (nm) ε (M^{-1} cm^{-1}) (in DMF): 640 (196), 397 (7333), 316 (9714). Molar conductance [Λ_M, (cm^2 Ω^{-1} mol^{-1})] in DMF: 160.

2.6.5. $[Ni_2L^{1e}](ClO_4)_2\cdot 2H_2O$ (L^{1e}–R = –phenyl) (**13**)

Anal. Calc. for $C_{28}H_{28}N_4O_2Ni_2(ClO_4)_2\cdot 2H_2O$: C, 41.78; H, 3.99; N, 6.98; Ni, 14.04. Found: C, 41.46; H, 3.78; N, 7.08; Ni, 13.76%. Selected IR ν (cm^{-1}) (using KBr): 3480, 1630, 1098. UV–Vis: λ_{max} (nm) ε (M^{-1} cm^{-1}) (in DMF): 650 (220), 384 (9390), 290 (sh). Molar conductance [Λ_M, (cm^2 Ω^{-1} mol^{-1})] in DMF: 165.

2.6.6. $[Ni_2L^{2a}](ClO_4)_2\cdot H_2O$ (L^{2a}–R = –$(CH_2)_2$–) (**14**)

Anal. Calc. for $C_{22}H_{22}N_4O_2Br_2Ni_2(ClO_4)_2\cdot H_2O$: C, 30.42; H, 2.79; N, 6.48; Ni, 13.52. Found: C, 29.99; H, 2.95; N, 6.28; Ni, 13.28%. Selected IR ν (cm^{-1}) (using KBr): 3420, 1635, 1090. UV–Vis: λ_{max} (nm) ε (M^{-1} cm^{-1}) (in DMF): 550 (267), 418 (5402), 330 (5944). Molar conductance [Λ_M, (cm^2 Ω^{-1} mol^{-1})] in DMF: 140.

2.6.7. $[Ni_2L^{2b}](ClO_4)_2\cdot CH_3OH$ (L^{2b}–R = –$(CH_2)_3$–) (**15**)

Anal. Calc. for $C_{23}H_{24}N_4O_2Br_2Ni_2(ClO_4)_2\cdot CH_3OH$: C, 32.15; H, 3.13; N, 6.28; Ni, 13.09. Found: C, 32.12; H, 2.85; N, 6.08; Ni, 13.20%. Selected IR ν (cm^{-1}) (using KBr): 3450, 1630, 1110. UV–Vis λ_{max} (nm) ε (M^{-1} cm^{-1}) (in DMF): 610 (183), 375 (5210), 315 (7689). Molar conductance [Λ_M, (cm^2 Ω^{-1} mol^{-1})] in DMF: 151.

2.6.8. $[Ni_2L^{2c}](ClO_4)_2\cdot H_2O$ (L^{2c}–R = –$(CH_2)_4$–) (**16**)

Anal. Calc. for $C_{24}H_{26}N_4O_2Br_2Ni_2(ClO_4)_2\cdot H_2O$: C, 32.15; H, 3.15; N, 6.25; Ni, 13.09. Found: C, 31.95; H, 2.99; N, 6.13; Ni, 12.98%. Selected IR ν (cm^{-1}) (using KBr) 3350, 1620, 1100. UV–Vis: λ_{max} (nm) ε (M^{-1} cm^{-1}) (in DMF): 620 (133), 385 (9381), 295 (sh). Molar conductance: [Λ_M, (cm^2 Ω^{-1} mol^{-1})] in DMF: 160.

2.6.9. $[Ni_2L^{2d}](ClO_4)_2\cdot CH_3OH\cdot H_2O$ (L^{2d}–R = –$(CH_2)_2$–NH–$(CH_2)_2$–) (**17**)

Anal. Calc. for $C_{24}H_{27}N_5O_2Br_2Ni_2(ClO_4)_2\cdot CH_3OH\cdot H_2O$: C, 31.82; H, 3.52; N, 7.51; Ni, 12.44 Found: C, 31.15; H, 3.50; N, 7.13; Ni, 11.92%. Selected IR ν (cm^{-1}) (using KBr): 3350, 1635, 1095. UV–Vis: λ_{max} (nm) ε (M^{-1} cm^{-1}) (in DMF): 650 (164), 394 (6198), 320 (4752). Molar conductance: [Λ_M, (cm^2 Ω^{-1} mol^{-1})] in DMF: 158.

2.6.10. $[Ni_2L^{2e}](ClO_4)_2\cdot CH_3OH$ (L^{2e}–R = phenyl) (**18**)

Anal. Calc. for $C_{26}H_{22}N_4O_2Br_2Ni_2(ClO_4)_2\cdot CH_3OH$: C, 34.85; H, 2.82; N, 6.02; Ni, 12.61. Found: C, 34.15; H, 2.48; N, 5.70; Ni, 13.45%. Selected IR ν (cm^{-1}) (using KBr): 3380, 1624, 1105. UV–Vis: λ_{max} (nm) ε (M^{-1} cm^{-1}) (in DMF): 650 (189), 382 (6419), 338 (6681). Molar conductance [Λ_M, (cm^2 Ω^{-1} mol^{-1})] in DMF: 155.

3. Results and discussion

3.1. Spectral analyses

The positive ion FAB mass spectra of the complexes show peaks corresponding to dipositive core $[Ni_2L]^{2+}$. Peaks corresponding to various mass units are given in Table 1. The mass spectrum of the complex $[Ni_2L^{1d}]$ is shown in Fig. 2. Conductivity studies of the complexes also show a conductance value in the range 140–165 Ω^{-1} mol^{-1} cm^2 consistent of dipositive charge of the complex.

IR spectra of the complexes $[NiL^1]$ and $[NiL^2]$ show a peak due to –HC=O around 1670 cm^{-1} whereas macrocyclic mononuclear complexes $[NiL^{1a-c}]$ and the binuclear complexes show a characteristic peak in the range 1625–1630 cm^{-1} due to ν(C=N) vibration [12]. All the binuclear complexes show broad perchlorate ion peak at 1110 and 620 cm^{-1} indicating the ionic nature of the complex.

All the binuclear nickel(II) complexes are soluble in DMF. The electronic spectra of the complexes (**9**–**18**) show a single weak d–d band in the region (550–670 nm) due to $^1A_1g \rightarrow {}^2A_1g$ associated with a square-planar [13] geometry around the Ni(II) ion. A red shift in the λ_{max} value of d–d band [14] with increase in the chain length between imine nitrogen has been observed. This red shift may be due to the distortion from planar geometry as the chain length increases. Moderately intense band observed in the region (360–400 nm) is associated with ligand to metal charge transfer transition while intense transition observed in the region (300–350 nm) is associated with the azomethine linkage [11,15].

3.2. Electrochemistry of the complexes

The electrochemical properties of the binuclear complexes were studied by cyclic voltammetry in DMF solution containing TBAP as supporting electrolyte in the potential range +1.3 to −1.3 V. The electrochemical data are given in Tables 2 and 3. The cyclic voltammograms of the complexes are shown in Fig. 3.

Generally the electrochemical properties of the complexes depend on a number of factors such as chelate ring/size [16,17], axial ligation [18,19], degree and distribution of unsaturation [16,20] and substitution pattern [16,21] in the chelate ring.

Table 1
Positive-ion FAB mass spectra of the binuclear complexes

Name of the complexes	Fragment	*m/z* (% intensity) [a]
$[Ni_2L^{1b}](ClO_4)_2\cdot H_2O$	$[Ni_2L^{1b}]^{2+}$	534 (58%)
	$[Ni_2L^{1b}](ClO_4)$	632 (85%)
	$[Ni_2L^{1b}]\cdot 2H_2O$	568 (40%)
$[Ni_2L^{1d}](ClO_4)_2\cdot H_2O$	$[Ni_2L^{1d}]^{2+}$	563 (65%)
	$[Ni_2L^{1d}](ClO_4)$	662 (78%)
	$[NiL^{1d}]\cdot H_2O$	525 (58%)
$[Ni_2L^{2a}](ClO_4)_2\cdot H_2O$	$[Ni_2L^{2a}]^{2+}$	520 (60%)
	$[Ni_2L^{2a}](ClO_4)$	619 (82%)
	$[NiL^{2a}]\cdot H_2O$	480 (48%)

[a] Relative to base peak.

3.3. Reduction process at negative potential

The electrochemical data of the complexes at negative potential is summarized in Table 2 and the cyclic voltammogram of the complexes is shown in Fig. 3. Reduction at negative potential is the usual trend observed for the phenoxide oxygen donor nickel(II) complexes. This is due to the 'hard' nature and negative influence of the phenoxide ligand. The cyclic voltammograms of the complexes show two quasireversible one electron reductions is evident from the criteria: the $E_{1/2}$ values are independent of scan rate; the ΔE_p increases with increasing scan rate (10, 20, 50, 100 mV s^{-1}) and is always greater than 60 mV; i_{pa}/i_{pc} is not equal at different scan rates. At slower scan rate (10 mV s^{-1}) the reoxidation peak is absent. Controlled potential electrolysis carried out for the complexes at 100 mV more negative than the first reduction potential consumed one electron per molecule ($n = 0.95$) and at 100 mV more negative than the second reduction potential consumed two electrons per molecule ($n = 1.92$). Thus, the following conversions take place at the electrode surface $M(II)M(II) \rightleftharpoons M(I)M(II) \rightleftharpoons M(I)M(I)$.

The reduction potential of the mononuclear complex $[NiL^{2a}]$ ($E_{pc} = -0.92$ V) is observed at less negative potential than the complex $[NiL^{1a}]$ ($E_{pc} = -1.10$ V). Similarly the first reduction potential of the binuclear complex $[Ni_2L^{2a}]$ ($E_{pc} = -0.80$ V) is observed at less negative potential than the complex $[Ni_2L^{1a}]$ ($E_{pc} = -1.0$ V). This is due to the reason that complexes containing electron-withdrawing substituent (Br) at the *para* position to the phenoxide oxygen in the phenyl ring are reduced at less negative potential than complexes with electron-donating substituent (CH_3). This may be due to the lesser electron density on the metal ions as a result of poor electron donating nature of the bromide ion. Similar trend has been observed for other methyl substituted complexes (**1**, **4**, **5**, **10**–**13**) and bromo substituted complexes (**2**, **7**, **8**, **15**–**18**). Literature reports, [22], also show that the complexes containing electron withdrawing group reduce at less negative potential than complexes, which contain electron donating substituent.

In the macrocyclic complexes reported in the present work there are two different compartments one has N_2O_2(amine) (piperazine nitrogen) and the other has N_2O_2 (imine) (azomethine nitrogen) linkage between phenoxide oxygen atom. For mononuclear complex

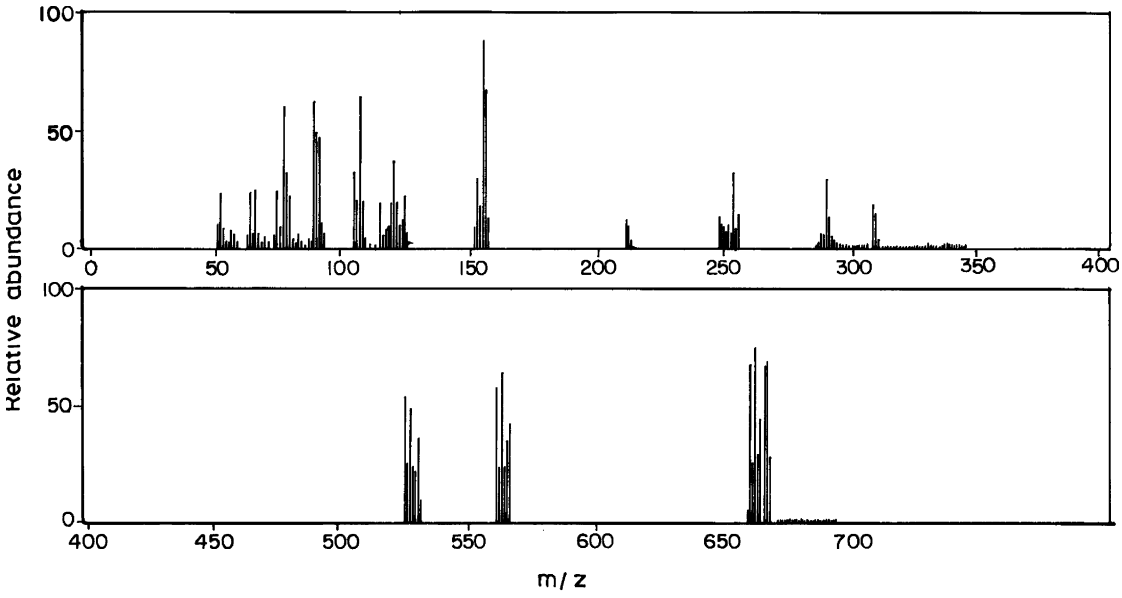

Fig. 2. Positive-ion FAB mass spectrum of the complex $[Ni_2L^{1d}]\cdot H_2O$ in *m*-nitrobenzylalcohol at room temperature.

$[NiL^1]$ the reduction potential is observed at −1.25 V and for mononuclear $[NiL^{1a-c}]$ complexes the reduction potential is observed around −1.10 to −0.95 V whereas for binuclear complexes $[Ni_2L^{1a-e}]$ the first reduction potential is observed around −1.0 to −0.78 V and the second reduction potential is observed around −1.2 V. The single reduction potential of the complexes $[NiL^{1a-c}]$ and the first reduction potential of the binuclear complexes $[Ni_2L^{1a-c}]$ are observed at nearly the same potential range. This shows that the reduction potential observed in the range (−1.0 to −0.70 V) is due to Ni^{2+} at imine compartment. The reduction potential of mononuclear complex $[NiL^1]$ and the second reduction potential of binuclear complexes $[Ni_2L^{1a-e}]$ are observed at nearly the same potential range. This shows that the reduction potential observed in this range (−1.2 V) is due to Ni^{2+} at amine (piperazine) compartment. This also shows that in $[NiL^1]$ the nickel ion is at amine compartment whereas in $[NiL^{1a}]$ the nickel ion is at imine compartment. Reports [23] show that the metal ion at unsaturated linkage is reduced first compared with saturated linkage. So, for our binuclear $[Ni_2L^{1a-e}]$ system, the first reduction potential observed from −1.0 to −0.78 V is due to Ni^{2+} at imine compartment and the second reduction potential observed at −1.2 V is due to Ni^{2+} at amine compartment. Similar trend has

Table 2
Electrochemical data for mono and binuclear complexes: (reduction at cathodic potential)

Complex	E^1_{pc} (V)	E^1_{pa} (V)	ΔE^1_p (mV)	$E^1_{1/2}$ (V)	E^2_{pc} (V)	E^2_{pa} (V)	ΔE^2_p (mV)	$E^2_{1/2}$ (V)
$[NiL^1]$	−1.25	−1.08	170	1.16				
$[NiL^2]$	−1.18	−1.0	180	1.09				
$[NiL^{1a}]\cdot H_2O$	−1.10	−0.92	180	−1.01				
$[NiL^{1b}]\cdot H_2O$	−1.03	−0.83	200	−0.93				
$[NiL^{1c}]\cdot H_2O$	−0.95	−0.77	180	−0.86				
$[NiL^{2a}]\cdot H_2O$	−0.92	−0.72	200	−0.82				
$[NiL^{2b}]\cdot H_2O$	−0.85	−0.67	180	−0.76				
$[NiL^{2c}]\cdot H_2O$	−0.80	−0.62	180	−0.71				
$[Ni_2L^{1a}](ClO_4)_2\cdot CH_3OH\cdot H_2O$	−1.00	−0.75	250	−0.87	−1.20	−1.00	200	−1.10
$[Ni_2L^{1b}](ClO_4)_2\cdot H_2O$	−0.95	−0.72	230	−0.83	−1.20	−1.02	180	−1.11
$[Ni_2L^{1c}](ClO_4)_2\cdot CH_3OH$	−0.80	−0.62	180	−0.71	−1.15	−0.95	200	−1.05
$[Ni_2L^{1d}](ClO_4)_2\cdot H_2O$	−0.78	−0.58	200	−0.68	−1.20	−1.00	200	−1.10
$[Ni_2L^{1e}](ClO_4)_2\cdot 2H_2O$	−0.92	−0.68	240	−0.80	−1.15	−0.90	250	−1.02
$[Ni_2L^{2a}](ClO_4)_2\cdot H_2O$	−0.80	−0.55	250	−0.67	−1.10	−0.90	200	−1.00
$[Ni_2L^{2b}](ClO_4)_2\cdot CH_3OH$	−0.75	−0.50	250	−0.62	−1.05	−0.88	170	−0.91
$[Ni_2L^{2c}](ClO_4)_2\cdot H_2O$	−0.72	−0.45	270	−0.58	−1.09	−0.83	260	−0.96
$[Ni_2L^{2d}](ClO_4)_2\cdot CH_3OH\cdot 2H_2O$	−0.72	−0.55	170	−0.63	−1.06	−0.86	200	−0.90
$[Ni_2L^{2e}](ClO_4)_2\cdot CH_3OH$	−0.68	−0.45	230	−0.56	−1.10	−0.92	180	−1.01

Measured by CV at 50 mV s^{-1} in DMF. *E* vs. Ag/AgCl conditions: glassy carbon working and Ag/AgCl reference electrodes; supporting electrolyte TBAP; concentration of TBAP 1×10^{-1} M, concentration of complex 1×10^{-3} M.

Table 3
Electrochemical data of the complexes (oxidation at anodic potential)

Complex	E^1_{pa} (V)	E^1_{pc} (V)	ΔE^1_p (mV)	$E^1_{1/2}$ (V)	E^2_{pa} (V)	E^2_{pc} (V)	ΔE^2_p (mV)	$E^2_{1/2}$ (V)
$[Ni_2L^{1a}](ClO_4)_2\cdot CH_3OH\cdot H_2O$	0.35	0.10	250	0.22	0.83	0.60	230	0.71
$[Ni_2L^{1b}](ClO_4)_2\cdot H_2O$	0.45	0.23	220	0.34	0.85	0.58	270	0.76
$[Ni_2L^{1c}](ClO_4)_2\cdot CH_3OH$	0.60	0.35	250	0.47	0.90	0.65	250	0.77
$[Ni_2L^{1d}](ClO_4)_2\cdot H_2O$	0.60	0.38	220	0.49	1.12	0.86	260	0.99
$[Ni_2L^{1e}](ClO_4)_2\cdot 2H_2O$	0.40	0.18	220	0.29	0.98	0.75	230	0.86
$[Ni_2L^{2a}](ClO_4)_2\cdot H_2O$	0.50	0.30	200	0.40	0.93	0.75	180	0.84
$[Ni_2L^{2b}](ClO_4)_2\cdot CH_3OH$	0.55	0.30	250	0.42	0.90	0.65	250	0.77
$[Ni_2L^{2c}](ClO_4)_2\cdot H_2O$	0.65	0.39	260	0.52	0.95	0.70	250	0.82
$[Ni_2L^{2d}](ClO_4)_2\cdot CH_3OH\cdot 2H_2O$	0.63	0.40	230	0.51	0.95	0.73	220	0.84
$[Ni_2L^{2e}](ClO_4)_2\cdot CH_3OH$	0.68	0.50	180	0.59	1.22	0.95	270	1.08

Measured by CV at 50 mV s^{-1} in DMF. E vs. Ag/AgCl conditions: glassy carbon working and Ag/AgCl reference electrodes; supporting electrolyte TBAP; concentration of TBAP 1×10^{-1} M, concentration of complex 1×10^{-3} M.

been observed for the complexes $[Ni_2L^{2a-e}]$. In $[Ni_2L^{2a-e}]$ the first reduction potential is observed from −0.80 to −0.68 V and the second reduction potential is observed around −1.10 V.

The reduction potential of the complexes is influenced by the chelate ring size. The reduction potential of the mononuclear complexes $[NiL^{1a-c}]$ shifts anodically (from $E_{pc} = -1.10$ to −0.95 V) as the chain length between imine nitrogen increases [24]. For binuclear complexes $[Ni_2L^{1a-d}]$ the first reduction potential shifts anodically (from $E_{pc} = -1.0$ to −0.78 V) as the chain length between imine nitrogen increases [24] (Fig. 3). Similar trend has been observed for the binuclear complexes $[Ni_2L^{2a-d}]$. Since as the chain length of the imine linkage increases, distortion around the metal center also increases, thereby favoring easier formation [16] of M(II) → M(I) to a greater extent. The electrochemical study indicates that the second reduction potential is observed at almost same potential around $E_{pc} = -1.2$ V. This also shows that the first reduction potential is due to the metal ion present in the imine compartment and the second reduction potential is due

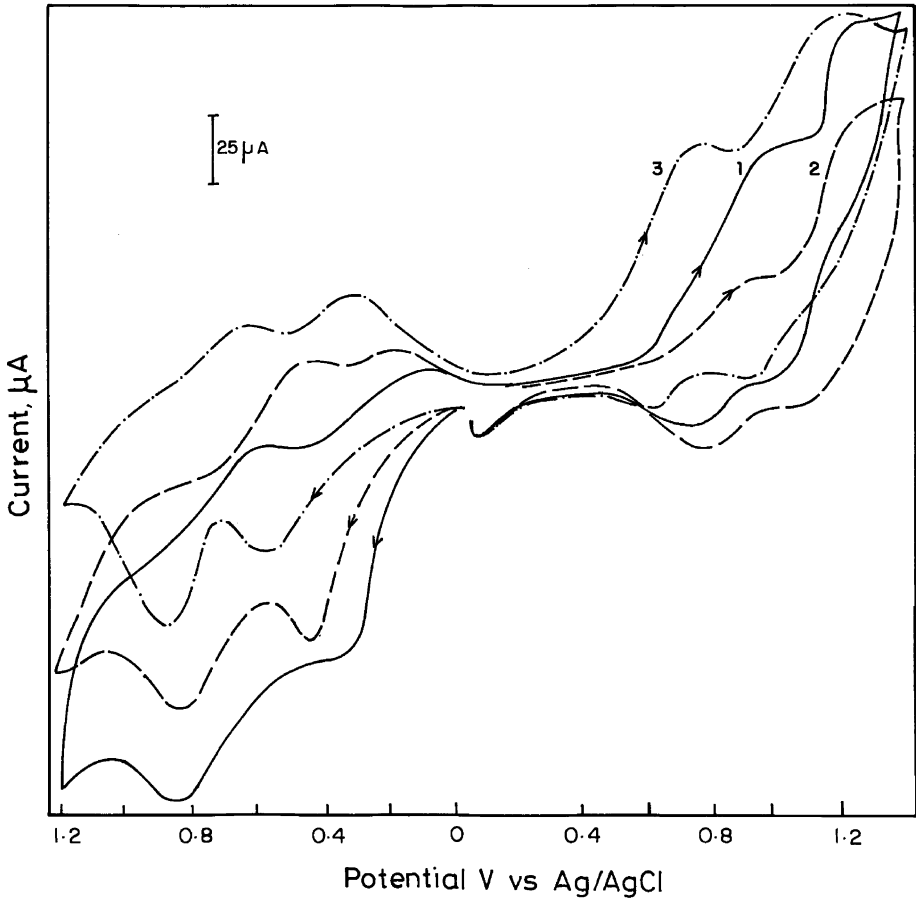

Fig. 3. Cyclic voltammogram of the complexes: $[Ni_2L^{1a}](ClO_4)_2$ (**1**), $[Ni_2L^{1b}](ClO_4)_2$ (**2**), $[Ni_2L^{1c}](ClO_4)_2$ (**3**).

to the metal ion in the amine compartment. The distortion around the metal ion at amine compartment is less than that around the metal ion at imine compartment. So, the second reduction potential due to the metal ion at amine compartment is observed at almost the same potential with increase in chain length of the imine linkage.

The reduction potential of nickel complex $[Ni_2L^{1e}]$ ($E_{pc} = -0.92$ V) is less than the complex $[Ni_2L^{1a}]$ ($E_{pc} = -1.0$ V). Similar trend has been observed for complexes $[Ni_2L^{2e}]$ ($E_{pc} = -0.68$ V) and $[Ni_2L^{2a}]$ ($E_{pc} = -0.80$ V). The electron withdrawing nature of the phenyl ring [25] attached to the imine nitrogen makes the deficiency of electron at the metal center causing the nickel(II) ion to reduce at less negative potential. The decrease in reduction potential is also due to the result of delocalization of the added electron density through the π-system of the phenylenediamine group.

3.4. Oxidation process at anodic potential

All the nickel complexes show two oxidation processes in the range +0.3 to +0.80 V. The cyclic voltammogram of the complexes is shown in Fig. 3 and the data are summarized in Table 3. The oxidation process is quasi-reversible in nature. Controlled potential electrolysis experiment indicates that the two oxidation peaks are associated with stepwise oxidation process at nickel(II) center, Ni(II)Ni(II)⇌Ni(III)Ni(II)⇌Ni(III)Ni(III). The first oxidation potential of the complexes $[Ni_2L^{1a-c}]$ shifts towards more positive value [16,24] (from $E_{pc} = +0.35$ to +0.60 V) as the chain length of imine linkage increases. This is because as the ring size increases, the planarity of the complex decreases and the electrochemical oxidation process occurs with difficult. Similar trend has been observed for complexes $[Ni_2L^{2a-c}]$. On comparing complex $[Ni_2L^{1a}]$ and $[Ni_2L^{1e}]$ it can be seen that as in the literature report, [26] complex $[Ni_2L^{1e}]$ oxidizes at slightly higher positive potential ($E_{pa} = 0.40$ V) than complex $[Ni_2L^{1a}]$ ($E_{pa} = 0.35$ V). Similar trend has been observed for complexes $[Ni_2L^{2a}]$ ($E_{pa} = 0.50$ V) and $[Ni_2L^{2e}]$ ($E_{pa} = 0.68$ V). This is because for complexes with aromatic diimine bridge, an increase in unsaturation will decrease the electron on the metal through delocalization, on to the ligand and this increases the difficulty to oxidize the metal ion.

References

[1] J. Nishio, H. Okawa, S. Ohtsuka, M. Tomono, Inorg. Chim. Acta 218 (1994) 27.

[2] (a) K.A. Margnus, M. Ton-That, J.E. Carpenter, Chem. Rev. 94 (1994) 727;
(b) D.E. Fenton, Adv. Inorg. Bioinorg. Mech. (1983) 187;
(c) D. Volkmer, B. Hommerich, K. Griesar, W. Haase, B. Krebs, Inorg. Chem. 35 (1996) 3792.

[3] (a) O. Kahn, Struct. Bonding (Berlin) 68 (1987) 89;
(b) P.A. Vigato, S. Tamburini, D.E. Fenton, Coord. Chem. Rev. 106 (1990) 25.

[4] (a) G.A. Melson (Ed.), Coordination Chemistry of Macrocyclic Compounds, Plenum Press, New York, 1979;
(b) A. Benicni, A. Bianchi, E. Garcia-Espana, Y. Jeania, M. Julve, V. Marcelino, M. Philoche-Levisalles, Inorg. Chem. 29 (1990) 962.

[5] V. Alexander, Chem. Rev. 95 (1995) 273.

[6] J. Lehn, Pure Appl. Chem. 52 (1980) 2441.

[7] (a) N.H. Pilikington, R. Robson, Aust. J. Chem. 23 (1970) 2225;
(b) H. Okawa, S. Kida, Bull. Chem. Soc. Jpn. 45 (1972) 1759;
(c) H. Okawa, S. Kida, Inorg. Nucl. Chem. Lett. 7 (1971) 751.

[8] S. Karunakaran, M. Kandaswamy, J. Chem. Soc., Dalton Trans. (1994) 1595.

[9] M. Marappan, V. Narayanan, M. Kandaswamy, J. Chem. Soc., Dalton Trans. (1998) 3405.

[10] J.C. Duff, J. Chem. Soc. (1941) 547.

[11] M. Yonemura, Y. Matsumura, H. Furutachi, M. Ohba, H. Okawa, D.E. Fenton, Inorg. Chem. 36 (1997) 2711.

[12] (a) G. Das, R. Shukala, S. Mandal, R. Singh, P.K. Baradwaj, J.V. Singh, K.H. Whitmire, Inorg. Chem. 36 (1997) 323;
(b) H. Wada, T. Aono, K. Motodo, M. Ohba, N. Matsumoto, H. Okawa, Inorg. Chim. Acta 246 (1996) 13.

[13] (a) T. Koga, H. Furutachi, T. Nakamura, N. Fukita, M. Ohba, K. Takahashi, H. Okawa, Inorg. Chem. 37 (1998) 989;
(b) T.C. Higgs, C.J. Carrano, Inorg. Chem. 36 (1997) 298;
(c) R. Bhalla, M. Helliwell, C.D. Garner, Inorg. Chem. 36 (1997) 2944;
(d) H. Okawa, S. Kida, Bull. Chem. Soc. Jpn. 45 (1972) 1759.

[14] B. Bosnich, J. Am. Chem. Soc. 90 (1968) 627.

[15] F.V. Lovecchio, E.S. Gore, D.H. Busch, J. Am. Chem. Soc. 96 (1974) 3104.

[16] G.K. Bareford, G.M. Freeman, D.G. Erver, Inorg. Chem. 86 (1986) 552.

[17] C. Kratky, R. Woditschatka, C. Angst, P.E. Johanson, J.C. Plaquevent, J. Schreiber, A. Eschenmoser, Helv. Chim. Acta 68 (1985) 1312.

[18] P.A. Connick, K.A. Macor, Inorg. Chem. 30 (1991) 4654.

[19] A.M. Tait, F.V. Lovecchio, D.H. Busch, Inorg. Chem. 16 (1977) 2206.

[20] J.A. Strecky, D.G. Pilsbury, D.H. Busch, Inorg. Chem. 19 (1980) 3148.

[21] (a) P. Amudha, M. Thirumavalavan, M. Kandaswamy, Polyhedron 18 (1999) 1363;
(b) J. Zubieta, J.C. Hayes, K.D. Karlin, in: K.D. Karlin, J. Zubieta (Eds.), Copper Coordination Chemistry. Biochemical and Inorganic Perspectives, Adenine, Guilderland, NY, 1983, p. 97.

[22] S.K. Mandal, L.K. Thompson, K. Nag, J.P. Charland, K.J. Gabe, Inorg. Chem. 26 (1987) 1391.

[23] H. Okawa, M. Tadokora, T.Y. Aretake, M. Ohba, K. Shindo, M. Mitsumi, M. Koikawa, M. Tomono, D.E. Fenton, J. Chem. Soc., Dalton Trans. (1993) 253.

[24] E. Gao, W. Bu, G. Yang, D. Liao, Z. Jiang, S. Yan, G. Wang, J. Chem. Soc., Dalton Trans. (2000) 1431.

[25] (a) R.K. Boggess, J.W. Hughes, W.W. Coleman, L.T. Taylor, Inorg. Chem. Acta 38 (1980) 183;
(b) A. Bottcher, T. Takeuchi, K.J. Hardcastle, T.J. Meade, H.B. Gray, D. Cwikel, M. Kapon, Z. Dori, Inorg. Chem. 36 (1997) 2498.

[26] F. Azevedo, C.T. Carrondo, B. Castro, M. Convery, D. Domingues, C. Freire, M.T. Duarte, K. Nielsen, I.C. Santos, Inorg. Chim. Acta 219 (1994) 43.